Photoionization from the $5p\ ^2P_{3/2}$ state of rubidium

Ali Nadeem* and S. U. Haq
National Institute of Lasers and Optronics (NILOP), P.O. Box Nilore, Islamabad 45650, Pakistan
(Received 28 February 2011; published 8 June 2011)

We report two-step photoionization studies from the $5p\ ^2P_{3/2}$ excited state of rubidium using two dye lasers simultaneously pumped by a common Nd:YAG laser in conjunction with a thermionic diode ion detector. The photoionization cross section at the first ionization threshold is measured as 18.8 ± 3 Mb and at excess energies of 0.013, 0.106, 0.229, and 0.329 eV is measured as 15, 13.6, 12.6, and 12.5 Mb, respectively. The measured value of the photoionization cross section at the threshold is used to calibrate the oscillator strengths of the $5p\ ^2P_{3/2} \rightarrow n\mathrm{d}\ ^2D_{5/2}$ ($22 \leqslant n \leqslant 52$) Rydberg transitions.

DOI: 10.1103/PhysRevA.83.063404 PACS number(s): 32.80.Fb, 32.70.Cs, 32.80.Ee

I. INTRODUCTION

The photoionization cross sections of atoms and oscillator strengths of transitions have been studied for decades because of the importance of these parameters in many fields of science such as astrophysics, plasma physics, and atmospheric science. Despite a long history of measurements and calculations, the measurements of photoionization cross sections of the excited states and oscillator strengths of the highly excited transitions are still in progress. We present here measurements of photoionization cross sections at and above the first ionization threshold and oscillator strengths of transitions from the $5p\ ^2P_{3/2}$ excited states of rubidium.

Photoionization cross sections from the low-lying states have been theoretically and experimentally investigated by few groups. Ambartzumian *et al.* [1] reported the photoionization cross sections from the $6p\ ^2P_{1/2}$ and $6p\ ^2P_{3/2}$ excited states of Rb using the saturation technique at 17 ± 0.4 Mb and 15 ± 0.4 Mb, respectively, ionized by the fundamental (≈694.3 nm) ruby laser. Wane [2] computed the rate coefficients for radiative recombination of Rb $n\ell$ states ($n \leqslant 20$, $\ell \leqslant 10$), and photoionization cross sections are calculated in the framework of the single-electron model. Cheret *et al.* [3,4] reported the collisional processes of highly excited Rb atoms and studied the excited states' photoionization cross sections of alkali-metal atoms. Aymar *et al.* [5] reported the most extensive work on the photoionization cross section for excited $n\ell$ states ($n \leqslant 20$, $\ell \leqslant 4$) of rubidium in the framework of a single-electron model. Systematic trends of nonhydrogenic behavior of photoionization cross sections for excited alkali-metal atoms have been discussed. The photoionization of cold trapped atoms was introduced by Dinneen *et al.* [6] to measure the photoionization cross section of the $5p\ ^2P_{3/2}$ state of rubidium at wavelengths of 413 and 407 nm as 13.6 and 12.5 Mb, respectively. Later, a similar technique was used in a vapor-filled magneto-optical trap (MOT) to measure the absolute photoionization cross section of Rb atoms from the $5p\ ^2P_{3/2}$ state at the 476.5-nm wavelength as 14.8 Mb by Gabbanini *et al.* [7]. Subsequently, Gabbanini *et al.* [8] reported the relative measurements of the partial photoionization cross sections of $\sigma_{5p,cd}$ and $\sigma_{5p,cs}$ as 12.6 and 2.2 Mb, respectively, with 20% uncertainty. In these measurements, the photoionization rates were determined from the change in the MOT loading rate. In the present paper, the photoionization cross sections from the $5p\ ^2P_{3/2}$ state are measured at the first ionization threshold and at the fourth energy position above the ionization threshold using the saturation technique, and a comparison is presented with previously reported data.

Most of the previously reported data on the ^2D states of rubidium are from two-photon absorption from the $5s^2S_{1/2}$ ground state. The reason may be that the ionization limit at about ≈33690 cm^{-1} is within the two-photon absorption range of continuous wave (cw) tunable dye lasers. Collins *et al.* [9] reported the highly excited $n\ ^2D$ states from $n = 9$–34 and $n\ ^2S$ states from $n = 11$–20 in the 460- to 650-nm range using multiphoton excitation with a tunable dye laser in conjunction with a space charge ionization detector. Yoshiaki and Stoicheff [10] reported the highly excited ^2D states from $n = 11$–32 of rubidium by Doppler-free photoabsorption spectroscopy using a cw dye laser. Ferguson and Dunn [11] observed the ^2S, ^2P, and ^2D series excited from the ground state and reported the term energies for the ^2S ($39 \leqslant n \leqslant 52$) and ^2D ($37 \leqslant n \leqslant 54$) states. Harvey and Stoicheff [12] reported the ^2D states of rubidium up to $n = 85$, only 16 cm^{-1} from the ionization limit, employing Doppler-free spectroscopy with counterpropagating beams from a cw dye laser. Stoicheff and Weinberger [13] reported the Doppler-free two-photon spectroscopy of $n\ ^2S \leftarrow 5\ ^2S$ and $n\ ^2D \leftarrow 5\ ^2S$ transitions from $n = 9$–116 and $n = 7$–124 respectively. In this work, a two-step photoionization spectrum is recorded $5p\ ^2P_{3/2} \rightarrow nd\ ^2D_{5/2}$ ($16 \leqslant n \leqslant 52$) for the calibration of oscillator strengths of these transitions.

The earliest data on the oscillator strengths and transition probabilities are based on the principal series and the few low-lying transitions [14–18]. Later, Niemax [19] reported the oscillator strengths of the electric quadrupole ($5s\ ^2S_{1/2} \rightarrow n\ ^2D_{5/2}$ and $5s\ ^2S_{1/2} \rightarrow n^2D_{3/2}$ ($4 \leqslant n \leqslant 9$) transitions of rubidium. Nilsen and Marling [20] reported the oscillator strengths of the $5s \rightarrow 4d$ first forbidden lines of rubidium at 516.5 nm as $8.06 \pm 0.48 \times 10^{-7}$ and $5.38 \pm 0.31 \times 10^{-7}$ for the $^2D_{5/2}$ and $^2D_{3/2}$ transitions respectively using the cw tunable dye laser. Langhoff *et al.* [21] computed the transitions probabilities between lowest ^2S, ^2P, and ^2D states of Na, K, Rb, and Cs using near Hartree-Fock-Slater basis sets. Zilitis [22] reported the oscillator strengths of the resonance

*drali_nadeem@yahoo.com; ali@nilop.edu.pk

transitions calculated using the Dirac-Fock method for the first 10 terms of the rubidium isoelectronic sequences. Klyucharev *et al.* [23] reported the relative oscillator strengths of the $^2S\ ^2P$ and $^2D\ ^2P$ transitions in optically excited Rb and Cs vapors from $n = 5$ to 9. Marek and Münster [24] reported the experimental lifetimes of the Rb atomic levels $n\ ^2S$, $n\ ^2P$, and $n\ ^2D$ up to $n = 12$. The most extensive work on the experimental and theoretical oscillator strengths from the $5p\ ^2P_{3/2} \rightarrow nd\ ^2D_{5/2}$ ($5 \leqslant n \leqslant 20$) transitions was reported by von der Goltz *et al.* [25]. The above literature survey show that the optical oscillator strengths of the $5p\ ^2P_{3/2} \rightarrow nd\ ^2D_{5/2}$ transitions are reported up to $n = 20$. In the present contribution, we extend the oscillator strengths of the above mentioned transitions up to $n = 52$.

II. EXPERIMENTAL DETAILS

The experimental technique is briefly described here; however, detailed description is available in previous papers [26,27]. A two-step excitation scheme to investigate the Rydberg state and to measure the photoionization cross section is shown in Fig. 1. The laser system is an injection-seeded Q-switch Nd:YAG (Spectra Physics) laser operating at a 30-Hz repetition rate with 7-ns pulse duration. The second and third harmonics were used to pump two Hanna-type dye lasers [28]. The first dye laser, operated with LDS 751 dye dissolved in dimethylsulfoxide (DMSO), was fixed at 780.24 nm, corresponding to the $5s\ ^2S_{1/2} \rightarrow 5p\ ^2P_{3/2}$ transition of rubidium. The second dye laser, operated with Coumarin 480 dye dissolved in methanol, was scanned from 33433 to 33648 cm^{-1} to record the $5p\ ^2P_{3/2} \rightarrow nd\ ^2D_{5/2}$, $ns^2S_{1/2}$ Rydberg transitions. For photoionization cross-sectional measurements, the second dye laser was charged with different dyes (Coumarin 460, 440, and Stilbene 420) to acquire the required wavelengths above the ionization threshold.

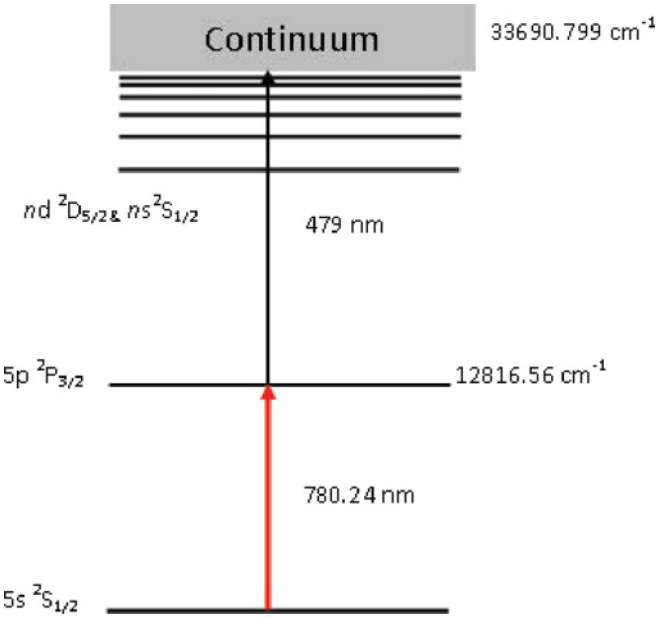

FIG. 1. (Color online) Two-step laser excitation scheme for the investigation of Rydberg states and photoionization cross-section measurements.

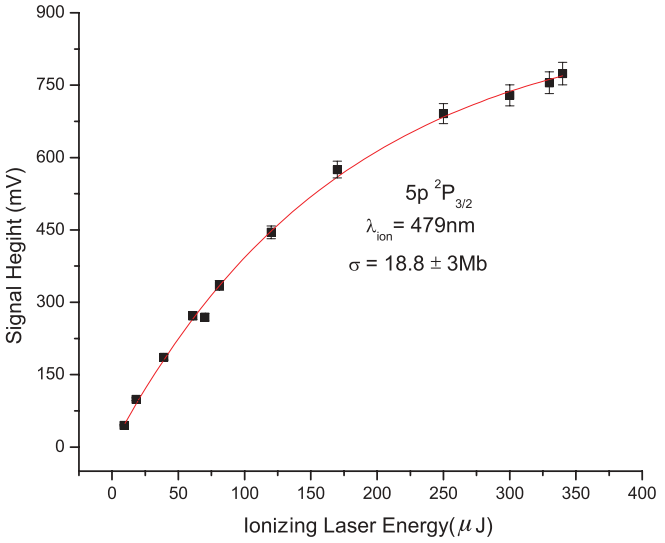

FIG. 2. (Color online) Photoionization signals from the $5p\ ^2P_{3/2}$ excited state plotted against the ionization laser energies. The solid line represents the least square fit of the Eq. (1). The absolute value of the cross section σ (Mb) from the $5p\ ^2P_{3/2}$ excited at 479-nm ionizing laser wavelength is extracted as 18.8 ± 3 Mb. The errors bar show pulse-to-pulse variation in the photoionizing signal.

The rubidium vapors were confined in a heat-pipe-like thermionic diode ion detector working in space-charge-limited mode. The heat pipe was operated with Ar as buffer gas; the temperature was kept at 375 K throughout the experiment and monitored with a thermocouple. A 0.25-mm-thick molybdenum wire, stretched axially along the tube, acts as a cathode, and the central heating zone is ≈20 cm long. About 1 g of rubidium was placed in the middle of the heat pipe. Both exciting and scanning dye laser beams were inserted into the thermionic diode from opposite sides and their spatial overlap was ensured in the central region. The change in the diode

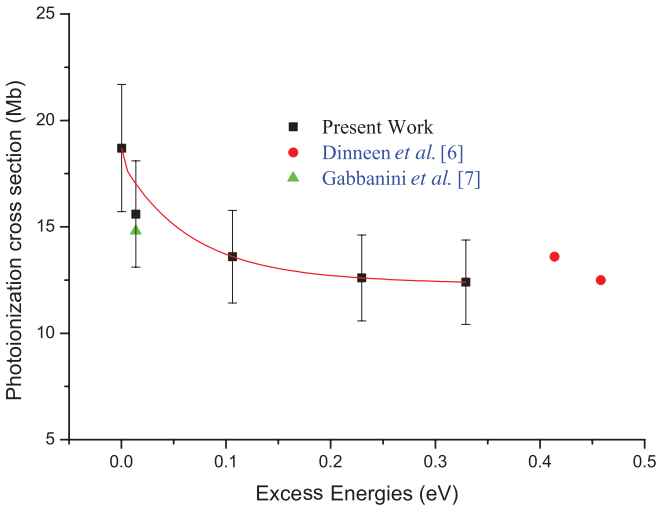

FIG. 3. (Color online) Plot of the photoionization cross section from the $5p\ ^2P_{3/2}$ excited state of rubidium on the excess energy and comparison with the earlier reported work. The solid line that passes through the experimental data represents the second-order exponential decay law.

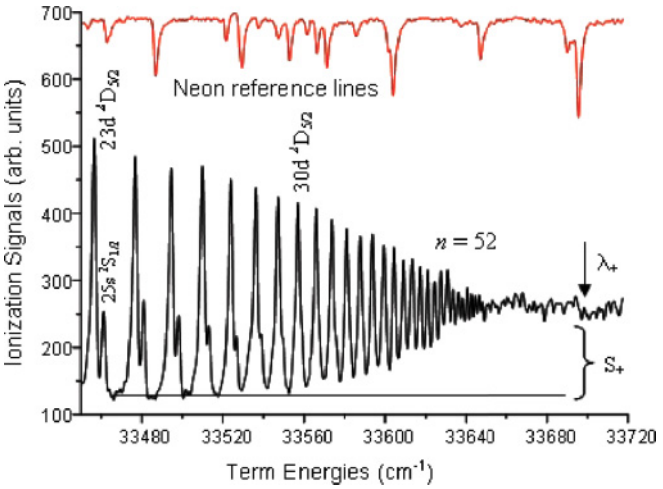

FIG. 4. (Color online) Portion of the spectrum showing the strongest $5p\ ^2P_{3/2} \rightarrow nd\ ^2D_{5/2}$ ($23 \leqslant n \leqslant 52$) transitions of rubidium and the low-intensity series is assigned as $ns\ ^2S_{1/2}$ from $n = 25$–29.

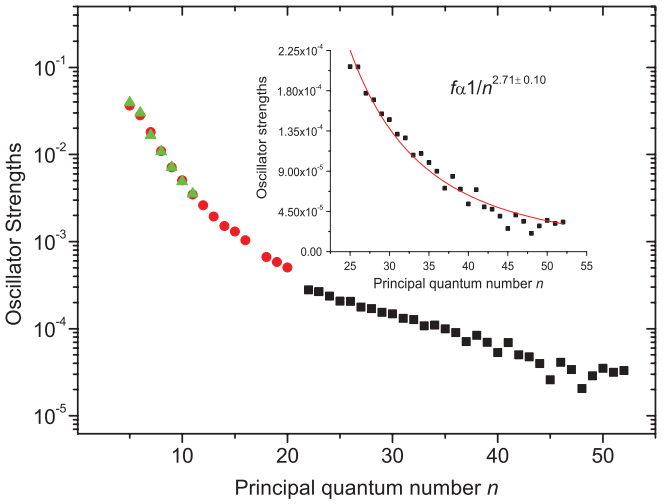

FIG. 5. (Color online) Plot of the oscillator strength distribution in the discrete region versus the principal quantum number n. The lower n data are taken from von der Goltz *et al.* [25] and Marek and Münster [24]. The inset in figure represents the trend of the f values with increasing principal quantum number n and varies as $1/n^{2.71}$.

current due to the photo-ion production was measured as a voltage drop across the 100-kΩ load resistor. The linearity of the detector was verified during the photoionization studies by configuring the detector for the strongest photoion signal corresponding to the maximum ionizing laser irradiance.

The wavelength calibration was achieved by simultaneously recording the optogalvonic spectra of neon by inserting a small portion of the scanning laser beam into a hollow cathode lamp, and another small fraction was passed through a 1-mm-thick solid etalon having 3.33 cm^{-1} free spectral range and was recorded through a photodiode. These signals were recorded simultaneously using three Box Car Averagers (SR-250) interfaced through a General Purpose Interface Bus (GPIB) card (NI 488). The data were recorded and stored on the computer for subsequent analysis. The level energies were determined, taking into account the neon reference wavelengths and the interference fringes from the etalon.

The photoionization cross section from the $5p\ ^2P_{3/2}$ excited state was measured using a two-step excitation scheme at and above the ionization threshold. The first dye laser (exciting laser) was fixed at 780.24 nm to populate the $5p\ ^2P_{3/2}$ excited state, and the second dye laser (ionizing laser) was fixed at the first ionization threshold of 479 nm and at four wavelengths (476.5, 460, 440, and 425 nm) above the ionization threshold. The photoionization cross sections have measured using the saturation technique as described in the following section.

III. RESULTS AND DISCUSSION

The absolute value of the photoionization cross section from the $5p\ ^2P_{3/2}$ excited state at and above the ionization threshold was measured using the saturation technique as described in [1,29,30]. This technique has been widely used for the measurement of the photoionization cross section of the excited states of alkali-metal atoms as well as for alkaline earths [31–35]. For the two-step photoionization process, the solution of the rate equations gives an expression that relates the absolute photoionization cross section at a particular wavelength of the ionizing laser:

$$N = N_{\rm ex}\left[1 - \exp\left(-\frac{\sigma U}{2\hbar\omega A}\right)\right]. \tag{1}$$

Here, $N_{\rm ex}$ (cm^{-3}) is the density of the excited atoms and A (cm^2) is the cross-sectional area of the ionizing laser beam. Additional parameters include U (joules), which is the energy per ionizing laser pulse, $\hbar\omega$ (joules) is the energy per photon of the ionizing laser beam, and σ (cm^2) is the absolute cross section for photoionization. All the parameters in Eq. (1) are known except the number density $N_{\rm ex}$ and photoionization cross section σ that can be extracted by the least square fit of Eq. (1) to the experimental data.

For the photoionization cross-section measurement from the $5p\ ^2P_{3/2}$ state, the first dye laser (exciting) promotes the ground-state atoms to the $5p\ ^2P_{3/2}$ intermediate state at 780.24 nm, and the second dye laser (ionizing) was fixed (479) at the $^1S_0$ threshold and at various energy positions above continuum. Both dye laser beams were inserted from opposite sides in a thermionic diode ion detector to ensure the spatial overlap of the laser beams; the ionizing laser beam was focused to a diameter much smaller than the exciting laser beam with a long focal length lens. The spot size of the ionizing laser beam was ≈2 mm, which is smaller than the spot size of the exciting laser, ≈5 mm. The spot size of the laser beams were determined at the point where the irradiance falls to $1/e^2$ of their axial peak value. Good alignment of the optical system produces a nearly diffraction-limited laser spot with large area of uniform intensity. The area of the overlap region in the confocal limit is calculated using the following relation [36]:

$$A = \pi r_o^2\left[1 + \left(\frac{\lambda_{\rm io}\ell}{\pi r_o^2}\right)\right]^2.$$

Here ℓ is taken as an effective length of the heating zone, $r_o = f\,\lambda_{\rm io}/\pi\, r$ is the beam waist, r is the radius of the spot size

TABLE I. The principal quantum number n, term energies, and f values of the $5p\ ^2P_{3/2} \rightarrow n\mathrm{d}\ ^2D_{5/2}$ Rydberg transitions of rubidium.

	$5\ p^2\mathrm{P}_{3/2} \rightarrow \mathrm{n}\ d^2\mathrm{D}_{5/2}$			
		f values		
n	Term energy (cm^{-1})	Present work	von der Goltz *et al.* [25]	Marek and Münster [24]
5			3.66×10^{-2}	30.94×10^{-2}
6			2.82×10^{-2}	3.00×10^{-2}
7			1.81×10^{-2}	1.66×10^{-2}
8			1.10×10^{-2}	1.08×10^{-2}
9			7.17×10^{-3}	7.11×10^{-3}
10			5.08×10^{-3}	4.89×10^{-3}
11			3.49×10^{-3}	3.54×10^{-3}
12			2.62×10^{-3}	–
13			1.95×10^{-3}	
14			1.51×10^{-3}	
15			1.31×10^{-3}	
16			1.04×10^{-3}	
17			–	
18			6.67×10^{-4}	
19			5.85×10^{-4}	
20			5.07×10^{-4}	
21				
22	33433.44	2.80×10^{-4}		
23	33456.59	2.67×10^{-4}		
24	33476.83	2.37×10^{-4}		
25	33494.50	2.07×10^{-4}		
26	33510.21	2.07×10^{-4}		
27	33523.89	1.77×10^{-4}		
28	33536.27	1.70×10^{-4}		
29	33547.23	1.54×10^{-4}		
30	33557.09	1.48×10^{-4}		
31	33565.93	1.31×10^{-4}		
32	33573.94	1.27×10^{-4}		
33	33581.23	1.08×10^{-4}		
34	33587.79	1.10×10^{-4}		
35	33593.85	9.97×10^{-5}		
36	33599.41	9.01×10^{-5}		
37	33604.51	7.11×10^{-5}		
38	33609.13	8.42×10^{-5}		
39	33613.42	7.00×10^{-5}		
40	33617.32	5.34×10^{-5}		
41	33621.04	6.94×10^{-5}		
42	33624.38	5.01×10^{-5}		
43	33627.50	4.74×10^{-5}		
44	33630.44	3.97×10^{-5}		
45	33633.23	2.59×10^{-5}		
46	33635.73	4.10×10^{-5}		
47	33638.15	3.40×10^{-5}		
48	33640.35	2.06×10^{-5}		
49	33642.44	2.88×10^{-5}		
50	33644.45	3.50×10^{-5}		
51	33646.28	3.15×10^{-5}		
52	33648.02	3.31×10^{-5}		

of the ionizing laser beam on the focusing lens, f is the focal length of the lens used, and λ_{io} is the wavelength of the ionizing laser. For the determination of cross section, the intensity of the ionizing laser beam was varied by placing the neutral density filters in the beam path, and the corresponding photoionization signal amplitude is measured on an oscilloscope. These values are incorporated in Eq. (1) to extract the photoionization cross section.

Figure 2 is a plot of photoionization signal versus the ionizing laser energy; in this figure, the ion yield first increases

up to a certain value of ionizing laser intensity and thereafter begins to saturate at higher intensity, but complete saturation has not been achieved. The complete saturation depends upon the state as well as on the intensity of the ionizing laser beam. In the present case, a solid line passing through the experimental data points is the least square fit of Eq. (1), which yield the photoionization cross section from the $5p\ ^2P_{3/2}$ excited state at the first ionization threshold as 18.8 ± 3 Mb. To verify our result, there is no experimental or theoretical data available on the photoionization cross section from the $5p\ ^2P_{3/2}$ state of rubidium at the first ionization threshold. However, the theoretical photoionization cross-sectional curves reported by Aymar *et al*. [5] from the $5p$ state are in the 12.5 to 14 Mb range at the ionization threshold.

We have further extended the photoionization cross-section measurements above the first ionization threshold under the same experimental conditions (temperature and buffer gas pressure) and technique. The photoionization cross section from the $5p\ ^2P_{3/2}$ excited state at excess energies 0.013, 0.106, 0.229, and 0.329 eV have been measured as 15, 13.6, 12.6, and 12.5 Mb, respectively, and data are plotted in Fig. 3. This figure also contains comparisons with data measured by some other groups. The present work is represented as squares; circles represent the photoionization cross section measured by Dinneen *et al.* [6], and triangles represent the data reported by Gabbanini *et al*. [7]. It is evident from the figure that the photoionization cross sections are large in the vicinity of ionization threshold and follow smooth decreasing trends at higher energies as theoretically computed [37,38]. Our results are in good agreement within the uncertainty of the previously reported data. The overall uncertainty in the measurement of photoionization cross section is 16%, which includes the uncertainty in the spatial profile of the ionizing laser beam (±10%), uncertainty in laser energy measurements with energy meter (±3%), pulse-to-pulse variation in laser energy (±3%), and uncertainty in photoionization signal amplitude measurement (± 2%).

For the determination of the oscillator strengths of the Rydberg transitions, a two-step photoionization spectrum was recorded from the $5p\ ^2P_{3/2}$ intermediate state. A portion of the photoionization spectra covering the energy range 33440 to 33720 cm^{-1} is shown in Fig. 4. The top trace shows the optogalvanic spectra of neon, and the bottom trace is the ionization signal from the thermionic diode ion detector. In a strict Russell-Saunders-coupling (LS-coupling) scheme, the accessible series from this intermediate level are $nd\ ^2D_{3/2,5/2}$ and $ns\ ^2S_{1/2}$. However, in this figure two series are evident: The dominating series is assigned as $nd^2D_{5/2}$ ($16 \leqslant n \leqslant 52$), whereas low-intensity transitions at the higher energy side of the main series are identified as $ns\ ^2S_{1/2}$ ($18 \leqslant n \leqslant 29$) series. The $ns\ ^2S_{1/2}$ series has been resolved from $nd\ ^2D_{5/2}$ series up to $n = 29$, and thereafter it loses its signal intensity. The identification of the $nd\ ^2D_{5/2}$ series was made according to the electric dipole intensity rules, in which transitions following $\Delta L = \Delta J = +1$ are expected to be the strongest, and hence among the $nd\ ^2D_{3/2,5/2}$ multiplet the signal intensity is dominated by the $nd\ ^2D_{5/2}$ series. Since for $5p\ ^2P_{2/3} \rightarrow nd\ ^2D_{3/2}$ transitions $\Delta l = \Delta L = 1$ and $\Delta J = 0$, this series possesses lower intensity, or as in the present experiment, is imbedded in the strong $nd\ ^2D_{5/2}$ transitions. Furthermore, the fine structure splitting of the $nd\ ^2D_{3/2,5/2}$ multiplets are 0.25 cm^{-1} and 0.20 cm^{-1} at $n = 12$ and 13, respectively, as reported in [38]. Therefore, in the present work, the dye laser line width was $\leqslant 0.3$ cm^{-1}, and it is not possible to resolve the fine structure components at higher n^* values because the fine structure splitting decreases as $1/n^3$ (n^* is the effective quantum number). A similar explanation is valid for the $5p\ ^2P_{3/2} \rightarrow ns\ ^2S_{1/2}$ series, as $\Delta\ell = \Delta L = 1$, but because $\Delta J = -1$ this series is expected to possess lower intensity than the $nd\ ^2D_{5/2}$ series. Furthermore, the identification of the $nd\ ^2D_{5/2}$ series was further supplemented by extrapolating the quantum defects of lower members of the series listed in the National Institute of Standards and Technology database [38]. The quantum defects have been calculated using the Rydberg relation:

$$E_n = E_\infty - \frac{\mathcal{R}}{(n - \delta_\ell)^2}.$$

Here E_n is the transition energy, E_∞ is the series convergence limit 33690.799 cm^{-1}, $\mathcal{R}$ is the mass-corrected Rydberg constant for rubidium 109736.605 cm^{-1}, and δ_ℓ is the quantum defect. The term energies of the observed series have been determined by adding the laser excitation energies to the $5\ p\ ^2P_{3/2}$ intermediate-state energy 12816.56 cm^{-1} [38], and the uncertainty in the measurement of term energies is approximately ±0.3 cm^{-1}. The higher members of the Rydberg series are used to determine the integrated signal intensity and wavelength of each transition for the determination of oscillator strength for the corresponding transition.

Having measured the photoionization cross section from the $5p\ ^2P_{3/2}$ state at first ionization threshold and acquiring the two-step photoionization spectra, the oscillator strengths of the $5p\ ^2P_{3/2} \rightarrow nd\ ^2D_{5/2}$ Rydberg transitions of rubidium have been determined using the experimental technique described by Mende and Kock [39]. This technique is valid for the determination of absolute oscillator strengths of Rydberg transitions for medium to high principal quantum numbers n, with the assumption that the collisional ionization probability of the transitions that lie within $k_B\ T$ (k_B is the Boltzmann constant, T is the temperature in Kelvin) is unity. A relation has been established between the f values of the Rydberg transitions and photoionization cross section at a particular frequency as

$$f_n = 3.77 \times 10^5 \frac{S_n \lambda_{1+}}{S_{1+} \lambda_n} \sigma^{1+}. \qquad (2)$$

Here f_n is the oscillator strength for the nth transition that is directly proportional to the photoionization cross section σ^{1+} measured at threshold ionizing wavelength λ_{1+}. The S_{1+} is the ion signal at the ionization threshold, and S_n is the integrated ion signal intensity of the nth transition.

After extracting the (S_{1+}, S_n, λ_{1+} and λ_n) parameters from Rydberg series and incorporating the threshold value of photoionization cross section (18.8 Mb), we have measured the oscillator strengths of the $5p\ ^2P_{3/2} \rightarrow nd\ ^2D_{5/2}$ ($22 \leqslant n \leqslant 52$) transitions using Eq. (2). The lower limit $n \geqslant 22$ is due to the condition that ionization probabilities of transitions should be unity; therefore, we have used only those transitions that lie well within k_BT (260 cm^{-1}) and assume that the ionization probabilities of all the transitions greater than $n = 22$ is unity. In the present

work, we have not performed any systematic studies related to the ionization probabilities of the highly excited states. However, Niemax [40] reported the ionization probabilities of the principal series of rubidium $5S \rightarrow nP$ ($n \geqslant 15$) in thermionic diode and the ionization probability of high-lying levels as unity, which also support our assumption. On the higher side, we have been limited to the $n = 52$ as the signal intensity of the Rydberg transitions becomes comparable to the background signal. Figure 5 shows the present and the reported f values of the $5p\ ^2P_{3/2} \rightarrow nd\ ^2D_{5/2}$ transitions versus the principal quantum number n. The solid squares represent the present work from $n = 22$ to 52, whereas the solid circles ($5 \leqslant n \leqslant 20$) are the results of von der Goltz *et al.* [25] and the triangles ($5 \leqslant n \leqslant 11$) are the f values extracted from the experimentally determined lifetime of nD levels reported by Marek and Münster [24]. A comparison is presented (see Fig. 5 in [25]). The inset in Fig. 5 shows a plot of the presently determined oscillator strengths versus the principal quantum number n indicating that the f values of an unperturbed Rydberg series scales as $1/n^{2.71}$. This smooth n dependence also supports our assumption that the ionization probability is taken as unity. The similar n^{-3} dependence of f values has been theoretically predicted by Duman and Shmatov [41] for the ionization rates of highly excited atoms colliding with ground-state atoms. The variations in the oscillator strengths at higher principal quantum number n are due to the variations in the intensities of the spectral lines that subsequently affect the f values of the transitions. The significant contribution to the ≈20% uncertainty in the measurement of the oscillator strengths is ≈16% in the measurement of the photoionization cross section and uncertainties in the measurement of the signal intensity, full width at half-maximum (FWHM), and the energy position of Rydberg transition. In Table I, the principal quantum number n, term energies of the Rydberg state, and f values of the above mentioned Rydberg transitions along with the previously reported data are presented.

In conclusion, we have measured the absolute photoionization cross section from the $5p\ ^2P_{3/2}$ state at the first ionization threshold and above the ionization limit. In addition, using the threshold value of the photoionization cross section, we have determined the optical oscillator strengths of the $5p\ ^2P_{3/2} \rightarrow nd\ ^2D_{5/2}$ ($22 \leqslant n \leqslant 52$) transitions of rubidium. Including the previously know oscillator strengths and the present work, a complete picture of the f values from $n = 5$ to 52 has been reported.

ACKNOWLEDGMENT

We thank the Pakistan Atomic Energy Commission (PAEC) for financial support.

[1] R. V. Ambartzumian, N. P. Furzikov, V. S. Letokhov, and A. A. Puretsky, Appl. Phys. **9**, 335 (1976).
[2] S. Wane, J. Phys. B: At. Mol. Phys. **18**, 3881 (1985).
[3] M. Cheret, L. Barbier, W. Lindinger, and R. Deloche, J. Phys. B: At. Mol. Phys. **15**, 3463 (1982).
[4] M. Cheret, W. Lindinger, L. Barbier, and R. Deloche, Chem. Phys. Lett. **88**, 229 (1982).
[5] M. Aymar, O. Robaux, and S. Wane, J. Phys. B: At. Mol. Phys. **17**, 993 (1984).
[6] T. P. Dinneen, C. D. Wallace, K.-Y. N. Tan, and P. L. Gould, Opt. Lett. **17**, 1706 (1992).
[7] C. Gabbanini, A. Lucchesini, and S. Gozzini, Opt. Commun. **25**, 141 (1997).
[8] C. Gabbanini, F. Ceccherini, S. Gozzini, and L. Lucchesini, J. Phys. B: At. Mol. Phys. **31**, 4143 (1998).
[9] C. B. Collins, S. M. Curry, B. W. Johnson, M.Y. Mirza, M. A. Chellehmalzadeh, J. A. Anderson, D. Popescu, and I. Popescu, Phy. Rev. A **14**, 1662 (1976).
[10] K. Yoshiaki and B. P. Stoicheff, J. Opt. Soc. Am. **66**, 490 (1976).
[11] A. I. Ferguson and M. H. Dunn, Opt. Commun. **23**, 227 (1977).
[12] K. C. Harvey and B. P. Stoicheff, Phys. Rev. Lett. **38**, 537 (1977).
[13] B. P. Stoicheff and E. Weinberger, Can. J. Phys. **57**, 2143 (1979).
[14] H. R. Kratz, Phys. Rev. **75**, 1844 (1949).
[15] O. S. Heavens, J. Opt. Soc. Am. **51**, 1058 (1961).
[16] I. V. Hertel and K. J. Ross, J. Phys. B: At. Mol. Phys. **2**, 484 (1969).
[17] E. Caliebe and K. Niemax, J. Phys. B: At. Mol. Phys. **12**, L45 (1979).
[18] E. Luc-Koenig and A. Bachlier, J. De. Phys. **39**, 1095 (1978).
[19] K. Niemax, J. Quant. Spectrosc. Radiat. Transfer **17**, 747 (1977).
[20] J. Nilsen and J. Marling, Quant. Spectrosc. Radiat. Transfer **22**, 327 (1978).
[21] S. R. Langhoff, C. W. Bauschlicher Jr., and H. Partridge, J. Phys. B: At. Mol. Phys. **18**, 13 (1985).
[22] V. A. Zilitis, Opt. Spectrosc. **103**, 895 (2007).
[23] A. N. Klyucharev, V. Yu. Sepman, and B. V. Dobrolezh, Opt. Spectrosc. **37**, 470 (1974).
[24] J. Marek and P. Münster, J. Phys. B: At. Mol. Phys. **13**, 1731 (1980).
[25] D. von der Goltz, W. Hansen, and J. Richter, Phys. Scr. **30**, 244 (1984).
[26] S. U. Haq and A. Nadeem, Phys. Rev. A **81**, 063432 (2010).
[27] A. Nadeem and S. U. Haq, Spectrochim. Acta, Part B **65**, 842 (2010).
[28] D. C. Hanna, P. A. Karkainen, and R. Wyatt, Opt. Quant. Elect. **7**, 115 (1975).
[29] C. E. Burkhardt, J. L. Libbert, J. Xu, and J. J. Leventhal, Phys. Rev. A **38**, 5949 (1988).
[30] L.-W. He, C. E. Burkhardt, M. Ciocca, and J. J. Leventhal, Phys. Rev. Lett. **67**, 2131 (1991).
[31] S. Hussain, M. Saleem, and M. A. Baig, Rev. A **75**, 022710 (2007).
[32] S. U. Haq, M. A. Kalyar, M. Rafiq, R. Ali, N. K. Piracha, and M. A. Baig, Phys. Rev. A **79**, 042502 (2009).
[33] S. U. Haq, R. Ali, M. A. Kalyar, M. Rafiq, and M. A. Baig, Eur. Phys. J. D **50**, 01 (2008).

[34] M. Rafiq, M. A. Kalyar, and M. A. Baig, J. Phys. B: At. Mol. Phys. **41**, 115701 (2008).
[35] W. Demtröeder, *Laser Spectroscopy*, 4th ed. Vol. 1 (Springer-Verlag, Berlin, 2008).
[36] D. W. Norcross, Phys. Rev. A **7**, 606 (1973).
[37] J. Lahiri and S. T. Manson, Phys. Rev. A **33**, 3151 (1986).
[38] NIST database [http://www.physics.nist.gov].
[39] W. Mende and M. Kock, J. Phys. B: At. Mol. Opt. Phys. **30**, 5401 (1997).
[40] K. Niemax, Appl. Phys. B **32**, 59 (1983).
[41] E. L. Duman and I. P. Shmatov, Sov. Phys.-JEPT **51**, 1061 (1980).